Isoscalar monopole and quadrupole strength of ^{16}O in an $\alpha + ^{12}$C cluster and symplectic mixed basis

Y. Suzuki
Physics Department, Niigata University, Niigata 950-21, Japan

S. Hara
Graduate School of Science and Technology, Niigata University, Niigata 950-21, Japan
(Received 8 July 1988)

The isoscalar monopole ($E0$) and quadrupole ($E2$) transition strength of ^{16}O is used to study how well the $\alpha + ^{12}$C cluster model works for explaining the strength distributions observed up to the isoscalar giant resonance region. The cluster model reproduces 54% of the $E0$ and 65% of the $E2$ energy weighted sum-rule strength. A symplectic basis, which naturally reproduces the sum rule, is mixed with the cluster basis to see how much of the missing strength is accounted for. A mixed basis calculation shows that the symplectic basis does not ruin the successful agreement of the cluster model with experiment obtained in the low-energy region and increases the strength by 30% for $E0$ and 20% for $E2$ below $E_x \leq 40$ MeV. It is predicted that both of the $E0$ and $E2$ strengths are split into two peaks in the giant resonance region with a greater spread over the excitation energy than expected.

I. INTRODUCTION

The microscopic cluster model has been developed to a fully mature stage with many applications to both structure and reaction problems. In the cluster model the constituent cluster wave functions are usually frozen to ground states approximated with lowest shell-model states, while the relative motion of the clusters carries arbitrary excitations. The remarkable success[1] of the cluster model when applied to light nuclei can be understood by the fact that some of the most important shell-model configurations can be expressed by exciting the relative motion degree of freedom. The $\alpha + ^{12}$C cluster model[2,3] for ^{16}O is a very good example to show that this is the case. In this model states of ^{16}O are described with an α particle orbiting around ^{12}C. The Pauli principle restricts configurations available for the relative motion of the clusters. The relative motion function was obtained in an orthogonality condition model approximation[4] which respects the Pauli principle. With the exception of the 10.96 MeV 0^- level the calculation reproduced almost all levels with isospin zero below 15 MeV in excitation energy and also reasonably reproduced the observed data of electric transition rates and α widths.

It is interesting to examine the cluster model at higher excitation energy. For this we focus on isoscalar quadrupole and monopole strength. The quadrupole strength, for example, is an important quantity associated with a quadrupole collectivity of the nucleus and its distribution has experimentally been investigated up to the giant resonance region. Since the isoscalar quadrupole and monopole operators are quadratic in nucleon position vectors, they can be rewritten as a sum of three terms convenient for the cluster model: two terms relevant to the respective clusters and a term for the relative motion. The latter is responsible for changing harmonic oscillator quanta of the relative motion by $2\hbar\omega$ and its effect is included in a basis of the cluster model. The part of the cluster-internal operators, however, induces the excitation of the clusters themselves, and its effect is not usually taken into account in the cluster model. A careful comparison with experiment of the $E2$ and $E0$ strength is therefore a good test of nuclear models, in particular, of the cluster model regarding the validity of an assumption of the frozen clusters. The energy weighted sum rule is particularly useful for this purpose.

The symplectic group Sp(6,R) (Ref. 5) has recently been developed as a microscopic theory of the nuclear collective motion. The generators of the Sp(6,R) group include all quadratic forms in nucleon coordinates and conjugate momenta and thus contain the monopole and quadrupole operators. The Sp(6,R) group is thus evidently expected to reproduce the energy weighted sum rule for their operators. The purpose of this paper is to investigate the extent to which the $\alpha + ^{12}$C cluster model of ^{16}O works for describing $E0$ and $E2$ strength up to high excitation energy and to clarify the role of the symplectic model when it is mixed with the cluster basis.

We do not repeat the details of the cluster model since they are fully described in Ref. 3. In Sec. II we give our basis wave functions for both models and remark on their relationship through the overlap of the wave functions. The overlap is needed to construct an orthonormal basis in the cluster-Sp(6,R) mixed-basis calculation. First we show the distributions of $E0$ and $E2$ strength obtained with the Sp(6,R) model in Sec. III, and then compare the results of the pure cluster and cluster-Sp(6,R) mixed-basis calculation with experment in Sec. IV. Section V gives a summary and discussion.

II. THE CLUSTER-SYMPLECTIC MIXED BASIS OF ^{16}O

The normalized $\alpha + ^{12}$C cluster wave functions are defined in an SU(3) coupled basis by

$$|[(04)\times(Q0)](\lambda\mu)\alpha\rangle=\{\sigma[(04)Q;(\lambda\mu)]\}^{-1/2}\mathcal{A}\{[\phi^{(00)}(\alpha)\times\phi^{(04)}(^{12}\mathrm{C})]^{(04)}\times\chi^{(Q0)}(\mathbf{R})\}_{\alpha}^{(\lambda\mu)}\ , \tag{1}$$

where the antisymmetrizer, $\mathcal{A}$, handles antisymmetrization between the clusters. The properly antisymmetrized internal wave functions, $\phi(\alpha)$ and $\phi(^{12}\mathrm{C})$, of the α and $^{12}\mathrm{C}$ clusters are assumed to be lowest possible Pauli-allowed states with SU(3) symmetry, (00) and (04), respectively. The relative motion function, χ, is an oscillator function in the (dimensionless) relative distance vector $\mathbf{R}$ between the clusters;

$$\mathbf{R}=\sqrt{3}[(\mathbf{r}_1+\cdots+\mathbf{r}_4)/4-(\mathbf{r}_5+\cdots+\mathbf{r}_{16})/12]\ .$$

It is assumed to have the same oscillator constant as the internal wave functions. The SU(3) symmetry of the total wave function is the resultant of the coupling of $(04)\times(Q0)$ and denoted by $(\lambda\mu)$ and its subgroup label α. The normalization constant $\sigma[(04)Q;(\lambda\mu)]$ is given by[6]

$$\sigma[(04)Q;(\lambda\mu)]=(\lambda+6)!(4-\mu)!\sum_{mnp}(-1)^{n+p}\frac{(4-n)!(Q-n)!}{n!(m-n)!(p-m)!(4-p)!(4-n-\mu)!(\lambda+6-n)!(Q-m)!}\left[\frac{1}{3}\right]^{m}\times\left[1-\frac{p}{3}\right]^{Q-m}\ . \tag{2}$$

The Pauli principle restricts the possible labels $(\lambda\mu)$ for low Q: Every $(\lambda\mu)$ state with $Q<4$ is Pauli-forbidden. Only the (00) state is Pauli-allowed for $Q=4$, and the three states with (42), (31), and (20) are Pauli-allowed for $Q=6$. In the calculations which follow we include all the $\alpha+^{12}\mathrm{C}$ cluster states up to $Q=18$ (14 $\hbar\omega$ excitation). The dimensions of the angular momentum subspaces for $J^{\pi}=0^{+}$, 2^{+}, and 4^{+} in the $\alpha+^{12}\mathrm{C}$ cluster model are 21, 46, and 57, respectively.

The normalized symplectic states based on the bandhead, $|\Gamma_{\sigma}=(00)\rangle$, of the 0 $\hbar\omega$ closed-shell configuration are given by

$$\begin{aligned}\bar{\Psi}\{(00)\Gamma_n\Gamma\alpha\}&=[\kappa^2(\Gamma_n)]^{-1/2}[P^{\Gamma_n}(\mathbf{A}^{\dagger})\times|\Gamma_{\sigma}=(00)\rangle]^{\Gamma}_{\alpha}\\&=[\kappa^2(\Gamma_n)]^{-1/2}\delta_{\Gamma,\Gamma_n}P^{\Gamma_n}_{\alpha}(\mathbf{A}^{\dagger})|(00)\rangle\ ,\end{aligned} \tag{3}$$

where $P^{\Gamma_n}_{\alpha_n}(\mathbf{A}^{\dagger})$ is the raising polynomial[7] of the raising generator, $\mathbf{A}^{\dagger}$, of the Sp(6,R) group. The normalization constants, $\kappa^2(\Gamma_n)$, are determined by a simple recursion relation[8]

$$\frac{\kappa^2([n_1'n_2'n_3'])}{\kappa^2([n_1n_2n_3])}=\tfrac{1}{2}[(\Delta n_1)^2+(\Delta n_2)^2+(\Delta n_3)^2]+\tfrac{1}{2}(\lambda_n+\mu_n-1)\Delta n_1+\tfrac{1}{2}(\mu_n-2)\Delta n_2-\tfrac{3}{2}\Delta n_3+n_3+22 \tag{4}$$

with the starting value of $\kappa^2([000])=1$, where $n_1'+n_2'+n_3'=n_1+n_2+n_3+2$, $\Delta n_i=n_i'-n_i$, $\lambda_n=n_1-n_2$, $\mu_n=n_2-n_3$. We include the symplectic states up to 14 $\hbar\omega$ excitation. The dimensions of the symplectic basis are 31, 39, and 34 for $J^{\pi}=0^{+}$, 2^{+}, and 4^{+}, respectively. The wave function of Eq. (1) with $Q=4$ and $(\lambda\mu)=(00)$ is the same as the bandhead of the Sp(6,R) model. The cluster model introduces excitations into the relative motion between the clusters with the internal structure of the clusters being kept fixed. In the symplectic model all the degrees of freedom are equally excited including both of the cluster-internal and cluster-relative motion. The cluster and symplectic wave functions of the same SU(3) symmetry ($N0$) have overlap[9,7]

$$\langle\bar{\Psi}\{(00)[N00](N0)\alpha\}|[(04)\times(N+4,0)](N0)\alpha\rangle=\frac{1}{9}\left[\left[1+\frac{31}{3^{N+2}}\right]^{-1}\frac{(N+4)(N+6)}{(N+1)}\frac{21!!(N+5)!!}{(N+21)!!}\right]^{1/2}\ . \tag{5}$$

For the 2 $\hbar\omega$ configurations of SU(3) symmetry (20) the overlap is 0.8076 and for configurations with large N it decreases rapidly.

The interaction matrix elements in the Sp(6,R) basis are evaluated by the method presented in Ref. 7. As also explained in Ref. 7, cluster-Sp(6,R) coupling matrix elements are evaluated by reducing them to ones between the Sp(6,R) bandhead and the cluster states, and the latter can be calculated by using matrix elements of unit SU(3) tensor operators. A part of the needed matrix elements of the unit tensor operators is given in Table II of Ref. 7. The evaluation of matrix elements in the cluster basis is done in the orthogonality condition model approximation[4] by transforming the SU(3) coupled cluster wave functions of Eq. (1) to the angular momentum coupled basis

$$|[(04)\times(Q0)](\lambda\mu)\kappa JM\rangle=\{\sigma[(04)Q;(\lambda\mu)]\}^{-1/2}\sum_{IL}\langle(04)I;(Q0)L\|(\lambda\mu)\kappa J\rangle\mathcal{A}\{[\phi^{(00)}(\alpha)\phi^{(04)}(^{12}\mathrm{C})]^{(04)}_{I}\chi^{(Q0)}_{L}(\mathbf{R})\}_{JM}\ , \tag{6}$$

where the SU(3)⊃R(3) Wigner coefficients are readily calculated from the computer code of Draayer and Akiyama.[10] The reason we use the orthogonality condition model approximation is that an exact calculation in the cluster model, although possible, does not reproduce both the binding energy of ^{16}O and the $\alpha+^{12}$C threshold energy at the same time. We have no two-nucleon potential available which is suited for the Sp(6,R)-cluster mixed basis calculation. The total energy curve of the closed-shell configuration against the oscillator parameter $b=[\hbar/m\omega]^{1/2}$ reaches an energy minimum of -125 MeV at $b=1.51$ fm for the Volkov No. 2 (V2) potential[11] with the Majorana exchange mixture $M=0.62$, while the corresponding values for the Brink-Boeker (B1) potential[12] are -93 MeV and 1.74 fm. Compare these with experiment (-128 MeV and 1.76 fm), where the experimental value of b is such that it reproduces the observed charge radius of 2.71 fm.[13] Apparently the V2 potential does not predict the correct size of ^{16}O and the B1 potential is too weak to reproduce the binding energy. In what follows we mainly use the B1 potential in the pure Sp(6,R) calculation and the V2 potential in the Sp(6,R)-cluster mixed-basis calculation. The oscillator parameter b is set to 1.51 fm when we use the V2 potential and to 1.74 fm when we use the B1 potential. The Coulomb potential is taken into account in our calculation.

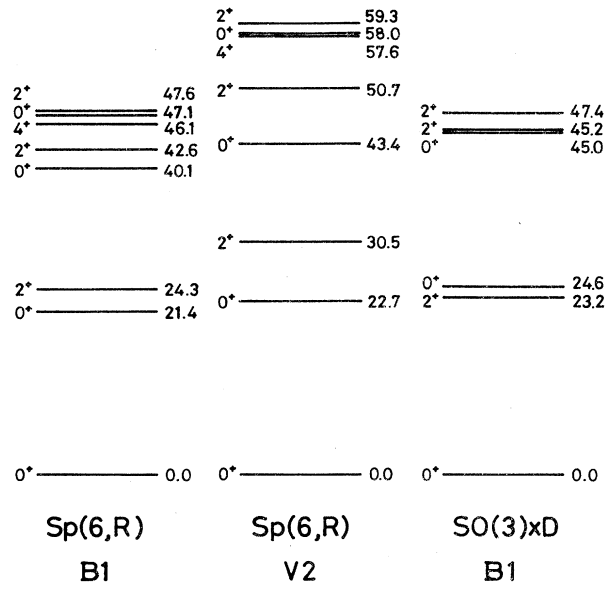

FIG. 1. The spectrum of ^{16}O calculated in the Sp(6,R) model. The SO(3)×D result is taken from Ref. 14. The two-nucleon potentials used are the Brink-Boeker B1 potential (Ref. 12) and the Volkov No. 2 potential (Ref. 11).

III. RESULTS OF CALCULATIONS IN THE Sp(6,R) BASIS

Figure 1 shows the energy spectrum of 0^+, 2^+, and 4^+ states in the pure Sp(6,R) basis calculation. It also shows the spectrum obtained by Vassanji and Rowe[14] in an SO(3)×D version of the Sp(6,R) model. The Sp(6,R) and SO(3)×D calculations using the B1 potential are very consistent: The ground-state energy and root-mean-square radius are -93.7 MeV and 2.63 fm, while in the SO(3)×D model they are -89.7 MeV and 2.70 fm when the Coulomb energy is estimated as 14.4 MeV. The spectrum is vibrational as expected, particularly for the B1 potential. As seen below, the 0_2^+ and 2_1^+ states are considered the isoscalar giant monopole (GMR) and quadrupole resonances (GQR). The Sp(2,R) model was applied to the breathing mode of ^{16}O (Ref. 15) and its energy of 22.9 MeV is slightly higher than the present value of 21.4 MeV. Five states lying above 40 MeV in excitation energy are the consequences of the monopole×monopole (0^+), monopole×quadrupole (2^+), and quadrupole ×quadrupole (0^+, 2^+, 4^+) excitations. The extent to which these states of two-phonon nature are split depends on the energy difference of the GMR and GQR. It is 3 MeV for the B1 potential and 8 MeV for the V2 potential.

Table I lists the properties of 0^+ and 2^+ states including the monopole and quadrupole strengths and the spectroscopic factors to proton and α emissions. It is clear that the 0_2^+ and 2_1^+ states can be interpreted as the isoscalar GMR and GQR. Inelastic scattering experiments of α particles from ^{16}O show that the isoscalar quadrupole strength is concentrated in the excitation energy of 16–28 MeV centered at 21 MeV.[16] Harakeh *et al.*[17] further indicate from the analysis of angular distributions that the state at 23.85 MeV may be a collective monopole state. The 0_2^+ and 2_1^+ states predicted by the Sp(6,R) model with the B1 potential are very consistent with these experiments. Of course, no single state is observed to have such a concentrated strength because of both the escape width to the continuum and the spreading width due to the coupling with noncollective states. The spec-

TABLE I. Properties of the 0^+ and 2^+ states of ^{16}O obtained in the Sp(6,R) model.

	E	$\lvert\langle 0_n^+\rvert\sum_p r_p^2\rvert 0_1^+\rangle\rvert$		S_α^2 (IL)		S_p^2 (jL)	
	(MeV)	(fm^2)	% $E0$ EWSR	(00)	(22)	($\frac{1}{2}$1)	($\frac{3}{2}$1)
0_1^+	-93.7	55.2		0.29	1.45	2.07	4.15
0_2^+	-72.2	10.0	88.7	0.08	0.35	0.18	0.35

	E	$B(E2;2_1^+\rightarrow 0_1^+)$		S_α^2 (IL)				S_p^2 (jL)			
	(MeV)	(e^2fm^4)	% $E2$ EWSR	(02)	(20)	(22)	(24)	($\frac{1}{2}$1)	($\frac{1}{2}$3)	($\frac{3}{2}$1)	($\frac{3}{2}$3)
2_1^+	-69.4	18.3	91.7	0.05	0.02	0.04	0.20	0.02	0.12	0.05	0.23

troscopic factors for α and proton channels show that the GMR has large decay amplitudes to $\alpha+{}^{12}\mathrm{C}(I^{\pi}=2^{+})$ with the orbital angular momentum $L=2$ and to $p+{}^{15}\mathrm{N}(j^{\pi}=\frac{3}{2}^{-})$ with $L=1$ and that the GQR has large amplitudes to $\alpha+{}^{12}\mathrm{C}(2^{+})$ with $L=4$ and to $p+{}^{15}\mathrm{N}(\frac{3}{2}^{-})$ with $L=3$. The decay scheme of the giant resonances is understood from the fact that the ground state is of almost pure closed-shell configuration (97%) and that the 2 $\hbar\omega$ Sp(6,R) state of SU(3) symmetry (20) is a dominant component of the giant resonances. To confirm this we derive formulas to calculate the spectroscopic factors of the 2 $\hbar\omega$ Sp(6,R) state of SU(3) symmetry (20) using the overlap formula between the symplectic and cluster states.

The reduced width amplitudes for α-particle emission are

$$y(R)=\langle\{[\phi_0^{(00)}(\alpha)\phi_I^{(04)}({}^{12}\mathrm{C})]_I Y_L(\hat{\mathbf{R}})\}_{JM}|\bar{\Psi}\{(00)[200](20)JM\}\rangle$$
$$=\langle(04)I;(60)L\|(20)J\rangle\{\sigma[(04)Q=6;(20)]\}^{1/2}\langle[(04)\times(60)](20)JM|\bar{\Psi}\{(00)[200](20)JM\}\rangle\chi_L^{(60)}(R)\ , \quad (7)$$

and the spectroscopic factors are easily obtained as

$$S_\alpha^2=\int_0^\infty[y(R)]^2R^2dR=\frac{560}{621}\langle(04)I;(60)L\|(20)J\rangle^2\ . \quad (8)$$

The spectroscopic factors for proton emission to the $p_{1/2}$ and $p_{3/2}$ hole states of ${}^{15}\mathrm{N}$ are calculated by transforming the channel wave function to a spin-isospin coupled basis

$$[\phi_{1/2,1/2-1/2}(p)\phi^{(01)}_{(1/21)j,1/21/2}({}^{15}\mathrm{N})]_{IM,T_z=0}=\sum_{ST}U(\tfrac{1}{2}\tfrac{1}{2}I1;Sj)\langle\tfrac{1}{2}-\tfrac{1}{2}\tfrac{1}{2}\tfrac{1}{2}|T0\rangle[\phi_{1/2,1/2}(N)\phi^{(01)}_{1/2,1/2}(A=15)]^{(01)}_{(S1)IM,T0}\ , \quad (9)$$

where $\phi_{1/2,1/2}(N)$ stands for the spin-isospin wave function of the nucleon and $\phi^{(01)}_{1/2,1/2}(A=15)$ the $0p$-hole wave function of the nucleus with mass number $A=15$. Only the $S=T=0$ component contributes to the overlap with the Sp(6,R) state so that the proton channel is effectively replaced with the state

$$[\phi_{1/2,1/2-1/2}(p)\phi^{(01)}_{(1/21)j,1/21/2}({}^{15}\mathrm{N})]_{IM,T_z=0}\rightarrow\delta_{I,1}(-1)^{j+1/2}\left[\frac{2j+1}{6}\right]^{1/2}\left[-\frac{1}{\sqrt{2}}\right][\phi_{1/2,1/2}(N)\otimes\phi^{(01)}_{1/2,1/2}(A=15)]^{(01)}_{IM}\ , \quad (9')$$

where the symbol $\otimes$ means the coupling of $S=0$ and $T=0$. The reduced width amplitudes for proton emission are thus

$$y(R')=(-1)^{j+1/2}\left[\frac{2j+1}{6}\right]^{1/2}\left[-\frac{1}{\sqrt{2}}\right]\langle(01)1;(30)L\|(20)J\rangle$$
$$\times\{\sigma[(01)3;(20)]\}^{1/2}\langle[(01)\times(30)](20)JM|\bar{\Psi}\{(00)[200](20)JM\}\rangle\chi_L^{(30)}(R')\ , \quad (10)$$

where $\mathbf{R}'=\sqrt{15/16}[\mathbf{r}_1-(\mathbf{r}_2+\cdots+\mathbf{r}_{16})/15]$ is the (dimensionless) relative distance vector between proton and ${}^{15}\mathrm{N}$. The spectroscopic factors are thus given by

$$S_p^2=\tfrac{16}{207}(2j+1)\langle(01)1;(30)L\|(20)J\rangle^2\ . \quad (11)$$

Here $|[(01)\times(Q0)](\lambda\mu)\alpha\rangle$ denotes the $ST=00$ coupled, normalized cluster wave function of the nucleon$+(A=15)$ system

$$|[(01)\times(Q0)](\lambda\mu)\alpha\rangle=\{\sigma[(01)Q;(\lambda\mu)]\}^{-1/2}$$
$$\times\mathcal{A}\{[\phi_{1/2,1/2}(N)\otimes\phi^{(01)}_{1/2,1/2}(A=15)]^{(01)}\times\chi^{(Q0)}(\mathbf{R}')\}^{(\lambda\mu)}_{\alpha}\ . \quad (12)$$

The normalization constant σ is given in Ref. 6:

$$\sigma[(01)Q;(Q-1,0)]=1-(-\tfrac{1}{15})^Q+\tfrac{16}{15}(3Q+8)(-\tfrac{1}{15})^{Q-1}\ ,$$
$$\sigma[(01)Q;(Q1)]=1-(-\tfrac{1}{15})^Q-\tfrac{16}{15}Q(-\tfrac{1}{15})^{Q-1}\ . \quad (13)$$

Table II lists the spectroscopic factors of the Sp(6,R) (20) state. Comparing Tables I and II confirms the dominance of this (20) state in the 0_2^+ and 2_1^+ states. Although the decays of the GMR and GQR seem to proceed with the greatest probability into the ${}^{12}\mathrm{C}(4^+)$ state with $L=4$ and 6, respectively, the penetration factors for this channel are so strongly suppressed that they are not the main decay modes of the giant resonances. Since the p_0 channel does not have a large spectroscopic factor and also the $p+{}^{15}\mathrm{N}(\frac{3}{2}^-)$ channel is energetically unfavored, the α_1 channel with $L=2$ and 4 is most favored in the decays of the GMR and GQR. Knöpfle *et al.*[18] measured the charged particle (c) decay of the GQR in an ${}^{16}\mathrm{O}(\alpha,\alpha'c)$ coincidence experiment and found that the dominant de-

TABLE II. Spectroscopic factors of the 2 $\hbar\omega$ Sp(6,R) state of SU(3) symmetry (20).

(20) 0^+	S_α^2 (IL)			S_p^2 (jL)	
	(00)	(22)	(44)	$(\frac{1}{2}1)$	$(\frac{3}{2}1)$
	0.090	0.39	0.43	0.15	0.31

(20) 2^+	S_α^2 (IL)							S_p^2 (jL)			
	(02)	(20)	(22)	(24)	(42)	(44)	(46)	$(\frac{1}{2}1)$	$(\frac{1}{2}3)$	$(\frac{3}{2}1)$	$(\frac{3}{2}3)$
	0.054	0.021	0.044	0.22	0.018	0.044	0.50	0.025	0.13	0.049	0.26

cay of the GQR proceeds through the α_1 channel. An analysis including both the spectroscopic factors and the transmission coefficients was done in Ref. 19 to account for the large α- vs proton-decay ratio of the GQR in ^{16}O.

IV. ISOSCALAR MONOPOLE AND QUADRUPOLE STRENGTHS IN ^{16}O

The $\alpha+^{12}$C cluster model succeeds in reproducing the energy spectrum, electric transition rates, and α widths up to the excitation energy of 10–15 MeV.[3] In Sec. III we have shown that the Sp(6,R) model predicts states that exhaust almost all of the monopole and quadrupole strengths. This naturally leads us to ask a few questions: (1) Does the cluster model work well for explaining the monopole and quadrupole strengths at the giant resonance region? (2) What influence does the mixing of the symplectic states have on the results of the cluster model? To clarify these points we have done a cluster-Sp(6,R) mixed-basis calculation for $J^\pi=0^+$ and 2^+. As noted in Sec. II the V2 potential does not reproduce the size of ^{16}O correctly leading to some drawbacks in the mixed-basis calculation. To compensate for these defects we introduce an artifice by hand: (1) We shift down all the energies of the Sp(6,R) states with $J^\pi=2^+$ by 6 MeV since the GQR predicted with the V2 potential is located too high as seen in Fig. 1. (2) The matrix elements for monopole and quadrupole strengths are sensitive to the size of nuclei. We correct the calculated matrix elements by multiplying by a factor proportional to the ratio, 1.76/1.51, of the harmonic oscillator size parameters following the reason mentioned in Sec. II. (3) The calculated excitation energies of the 0^+ and 2^+ states are read in such a way that the 0_2^+ and 2_1^+ states calculated fit the observed values when we calculate the percentage of monopole and quadrupole strengths compared to the energy weighted sum rule (EWSR).

Figure 2 compares the isoscalar monopole strength obtained using the V2 potential in the pure cluster, Sp(6,R) and cluster-Sp(6,R) mixed calculations. The EWSR for the isoscalar monopole strength is given by

$$S_0 \equiv \sum_n (E_n - E_0)|\langle 0|\sum_p r_p^2|n\rangle|^2 = \frac{\hbar^2}{2m} A\langle r^2\rangle_0 . \quad (14)$$

The cluster model reproduces the observed monopole strength of the two low-lying states at 6.05 and 12.05 MeV except for the state at 14.03 MeV.[3] It is remarkable that the cluster model predicts a level with large monopole strength at about 22 MeV. The wave function of the level consists of the 2 $\hbar\omega$ (20) and (42) states (34.5%), admixed with the higher excited configurations (50.0%) of SU(3) symmetry (40), (60), (80),. . . . The accumulated energy weighted sum of the cluster model amounts to 50% of the $E0$ EWSR below 40 MeV in excitation energy. The cluster-Sp(6,R) mixed basis calculation shows that the energy spectrum below 20 MeV does not change very much and that the Sp(6,R) components increase by 30% the percentage of the energy weighted sum existing above the excitation energy of 20 MeV compared to the case of the pure cluster model. This seemingly small increase is due to the large overlap of the cluster and Sp(6,R) states of SU(3) symmetry (20) as noted in Sec. II and due to the near degeneracy of the two levels lying at 22 MeV. The mixed calculation suggests that a large percentage of the $E0$ EWSR spreads over the region of 20–30 MeV in excitation energy.

Figure 3 displays the isoscalar quadrupole strength calculated with the V2 potential. The EWSR for the isoscalar quadrupole strength is given by

$$S_2 \equiv \sum_n (E_n - E_0) B(E2; 2_n^+ \to 0) = \frac{5}{16\pi}\frac{e^2\hbar^2}{m} A\langle r^2\rangle_0 . \quad (15)$$

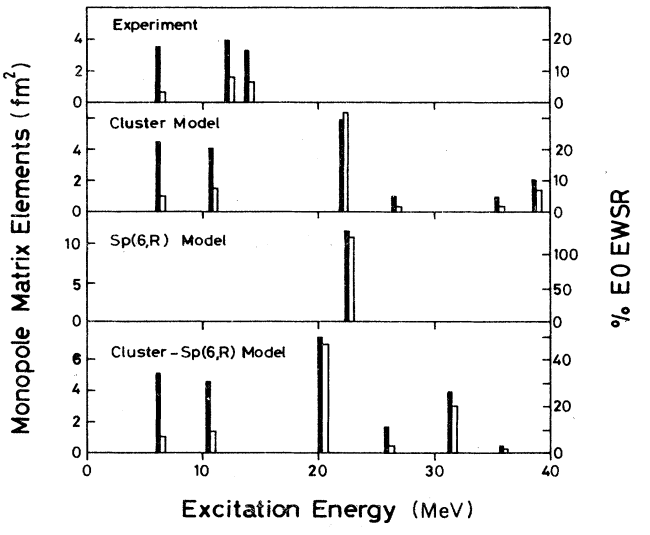

FIG. 2. The distribution of isoscalar monopole strength in ^{16}O. The experimental data are taken from Ref. 13. The bold lines denote the monopole matrix elements and the open rectangles denote the percentages of the energy weighted strength to the $E0$ EWSR.

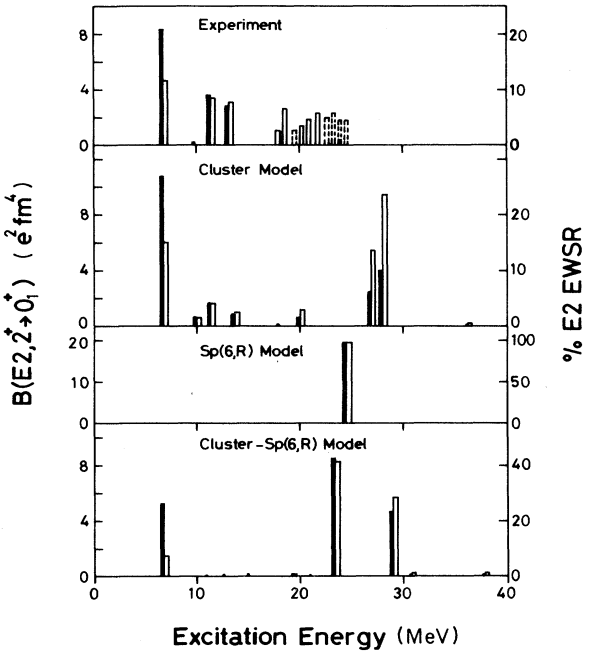

FIG. 3. The distribution of isoscalar quadrupole strength in ^{16}O. The experimental data are taken from Ref. 17. The bold lines denote the $B(E2)$ values and the open rectangles denote the percentages of the energy weighted strength to the $E2$ EWSR.

The observed energy weighted sum below 15 MeV accumulates to 30% of the $E2$ EWSR. The cluster model nicely reproduces the excitation energies of the low-lying 2^+ states, although the $B(E2)$ values are smaller than experiment for the states at 11.52 and 13.02 MeV. The cluster model further predicts that a large percentage ($\sim$40%) of the EWSR exists in the excitation energy region of 20–30 MeV, giving 60% of the $E2$ EWSR in total. The cluster-Sp(6,R) mixed-basis calculation shows that the $B(E2)$ strength of the low-lying 2^+ states is reduced compared to the pure cluster model calculation but the accumulated energy weighted sum increases by 20% of the EWSR. The $B(E2)$ strength observed experimentally shows diverse results, depending on the type of experiments as listed in Table VII of Ref. 17. The present result is not in contradiction with the (α,α') experiment. It is noted that, as in the case of the monopole strength, there exist two peaks with large quadrupole strength at 23 and 29 MeV. The α and proton spectroscopic factors of these states have been calculated and it is confirmed again that these states mainly decay through the α_1 channel. The needed overlap matrix elements of $\alpha+^{12}$C and $p+^{15}$N cluster wave functions are given in the Appendix.

The splitting of the isoscalar giant resonances is caused by a mixing of the Sp(6,R) and cluster states. To understand this we consider the simplest model. Assume that the ground state is described with a closed-shell configuration. Then the $2\hbar\omega$ Sp(6,R) state of SU(3) symmetry (20) has maximum $B(E2)$ strength to the ground state

$$|\langle 0|||Q|||\bar{\Psi}\{(00)[200](20)\}\rangle|^2=138\frac{15}{16\pi}\ , \tag{16}$$

where $Q_m=\sum_i r_i^2 Y_{2m}(\hat{\mathbf{r}}_i)$ is the quadrupole operator and the triple bar means SU(3), $R(3)$ reduced matrix element. The $\alpha+^{12}$C cluster state of the same SU(3) symmetry has $B(E2)$ strength to the ground state

$$|\langle 0|||Q|||[(04)\times(60)](20)\rangle|^2=90\frac{15}{16\pi}\ . \tag{17}$$

These state have a large overlap, however, and the cluster state orthogonalized to the Sp(6,R) state has exactly vanishing $B(E2)$ strength. [It is easy to check this by using Eq. (5).] The splitting of $B(E2)$ strength must therefore be a consequence of the coupling of the Sp(6,R) and cluster states. The actual calculation shows that the ground state is not a pure closed-shell configuration but contains the excited configurations appreciably and that the cluster configurations with higher oscillator excitations contribute to building up the $B(E2)$ strength. However, experiments[16–18,20–22] done up to now to study the isoscalar GQR of ^{16}O do not indicate clear evidence for its splitting, presumably because the energy region investigated is too limited to low energies. A recent experiment[23] has shown that the GQR of ^{40}Ca, the doubly magic nucleus, is split into two parts, one lying at 13.5±1.5 MeV with 40% strength of the EWSR and the other at 18±2 MeV with 50% strength. Shell-model[19,24] and RPA (Ref. 25) calculations predict only one peak at about 18 MeV. We think that an argument similar to ^{16}O can be applied to explaining the splitting of ^{40}Ca. In fact, the overlap of the corresponding states, the Sp(6,R) and $\alpha+^{36}$Ar cluster states,[26] of SU(3) symmetry (20) in ^{40}Ca is as large as 0.7577, and the ratio of their $B(E2)$ strengths to the ^{40}Ca core is 1:0.57.

V. SUMMARY AND DISCUSSION

An $\alpha+^{12}$C cluster model has been worked out for ^{16}O to investigate the distribution of the $E0$ and $E2$ strength up to the giant resonance region. We have used the orthogonality condition model approximation as a practical means for solving the equation of the relative motion of the clusters. We have used the Volkov No. 2 potential to obtain the $\alpha-^{12}$C potential via the folding procedure. Since the Volkov potential does not reproduce the saturation property of the nucleon density, we have corrected the calculated $E0$ and $E2$ matrix elements using a factor which is determined by the size parameter of harmonic oscillator functions. The cluster model nicely reproduces the $E0$ and $E2$ strength in the low-energy region as shown in a previous calculation and accounts for more than 50% of the sum rule value below 40 MeV in excitation energy. An Sp(6,R) model is a microscopic collective model for monopole and quadrupole degrees of freedom. An Sp(6,R) basis has been mixed with the cluster basis in order to see how much it affects the results of the cluster model and how much it increases the $E0$ and $E2$ strength. A mixed-basis calculation has shown that the effect of the Sp(6,R) basis is not very large at low excitation energy and that the Sp(6,R) basis increases the strength by 30% for $E0$ and 20% for $E2$ below 40 MeV.

These are in contrast with the case of ^{20}Ne. The $\alpha+^{16}$O cluster model for ^{20}Ne predicts a small percentage of the sum rule and its extension to include the excitation of ^{16}O as done in Ref. 27 accounts for, at most, 30% of the sum rule. The Sp(6,R) basis, however, greatly enhances the $E0$ and $E2$ strength, and the $\alpha+^{16}$O cluster-Sp(6,R) mixed-basis calculation[8] exhausts the sum rule. The reason for this contrast seems for one thing that, as expected from cluster model study, the ground state of ^{16}O contains admixtures of components from other symplectic bands more than the ground state of ^{20}Ne and for another the difference of the overlap of the cluster and symplectic wave functions with 2 $\hbar\omega$ excited configurations: The overlap is 0.808 for ^{16}O but 0.686 for ^{20}Ne. It is also interesting that the distributions of the energy weighted strength in the mixed-basis calculation for ^{16}O extend over higher excitation energy than expected and show two strong peaks at 20 and 32 MeV for $E0$ and at 23 and 29 MeV for $E2$, respectively. No experiment has so far given evidence for the splitting of the isoscalar giant resonances of ^{16}O, but the report that the distribution of the $E2$ strength of ^{40}Ca is found to be split encourages experimental effort to study that point.

The cluster-symplectic mixed-basis calculation raises an important question about the choice of appropriate effective interactions. In the cluster model we require that the effective interaction reproduce the binding energies of the constituent clusters and give a reasonable intercluster potential as inferred from phenomenological potentials. The appropriate effective interaction in the symplectic calculation must predict correctly the size and compressibility of the nucleus which are essential to the properties of the giant resonances. As shown in Ref. 8 and in this paper neither the Volkov nor the Brink-Boeker interaction satisfies both the requirements. Probably no such effective interaction is available in so far as it is state independent. We have to introduce a state or density dependence in the effective interaction as implied by G-matrix calculations.

This work has been done as a part of the annual research project "Molecular Aspects in High Excitation Energy Region and Mechanism of Heavy-Ion Reactions, 1987" supported by the Research Institute for Fundamental Physics, Kyoto University.

APPENDIX

We need to know the overlap of $\alpha+^{12}$C and $p+^{15}$N cluster wave functions for the calculation of the spectroscopic factor to the $p+^{15}$N channel. As the $\alpha+^{12}$C cluster wave function is spin-isospin scalar ($ST=00$), only the ST scalar part of the $p+^{15}$N cluster wave function contributes to the overlap as shown in Eqs. (9) and (9′). The needed overlap

$$\mathcal{O}^{Q(\lambda\mu)}=\langle\{[\phi_{1/2,1/2}(N)\otimes\phi^{(01)}_{1/2,1/2}(A=15)]^{(01)}\times\chi^{(Q-3,0)}(\mathbf{R}')\}^{(\lambda\mu)}_{\alpha}|\mathcal{A}|\{[\phi^{(00)}(\alpha)\times\phi^{(04)}(^{12}\mathrm{C})]^{(04)}\times\chi^{(Q0)}(\mathbf{R})\}^{(\lambda\mu)}_{\alpha}\rangle \tag{A1}$$

can be derived from the generating function

$$F_{\alpha'\alpha}(\overline{\mathbf{K}},\mathbf{K}^*)=\langle[\phi_{1/2,1/2}(N)\otimes\phi^{(01)}_{1/2,1/2}(A=15)]^{(01)}_{\alpha'}A(\overline{\mathbf{K}},\mathbf{R}')^*|\mathcal{A}|[\phi^{(00)}(\alpha)\times\phi^{(04)}(^{12}\mathrm{C})]^{(04)}_{\alpha}A(\mathbf{K}^*,\mathbf{R})\rangle\ , \tag{A2}$$

where

$$\begin{aligned}A(\mathbf{K},\mathbf{R})&=\pi^{-3/4}\exp[-\tfrac{1}{2}\mathbf{K}\cdot\mathbf{K}+\sqrt{2}\mathbf{K}\cdot\mathbf{R}-\tfrac{1}{2}\mathbf{R}\cdot\mathbf{R}]\\&=\sum_{Q\alpha}P^{(Q0)}_{\alpha}(\mathbf{K})[\chi^{(Q0)}_{\alpha}(\mathbf{R})]^*\end{aligned} \tag{A3}$$

is the kernel function which generates the Bargmann transform, $P^{(Q0)}_{\alpha}(\mathbf{K})$, of the harmonic oscillator function, $\chi^{(Q0)}_{\alpha}(\mathbf{R})$, in the space of the single three-dimensional variable $\mathbf{R}$. By including the center-of-mass motion degree of freedom and converting the matrix element of Eq. (A2) to one involving integration over all $A=16$ variables it is possible to convert $F_{\alpha'\alpha}(\overline{\mathbf{K}},\mathbf{K}^*)$ to the calculation of the standard form involving the Slater determinants,

$$\begin{aligned}F_{\alpha'\alpha}(\overline{\mathbf{K}},\mathbf{K}^*)=\exp[-\sqrt{1/45}\overline{\mathbf{K}}\cdot\mathbf{K}^*]\langle A(\sqrt{16/15}\overline{\mathbf{K}},\mathbf{r}_1)^*[\phi_{1/2,1/2}(N)\otimes\psi^{(01)}_{1/2,1/2}(A=15)]^{(01)}_{\alpha'}|\\\times\mathcal{A}|A(\sqrt{1/3}\mathbf{K}^*,\mathbf{X}_{\alpha})[\phi^{(00)}(\alpha)\times\psi^{(04)}(^{12}\mathrm{C})]^{(04)}_{\alpha}\rangle\ ,\end{aligned} \tag{A4}$$

where $\mathbf{X}_{\alpha}=(\mathbf{r}_1+\cdots+\mathbf{r}_4)/\sqrt{4}$ is the center-of-mass coordinate of the α particle, and the functions ψ are the shell-model wave functions centered at the origin. The subgroup labels α and α' can be chosen arbitrarily but the choice of $\alpha'=1\frac{1}{2}\frac{1}{2}$ and $\alpha=422$ in the Elliott SU(2)×U(1) labels ($\epsilon\Lambda M_{\Lambda}$) makes the calculation of Eq. (A4) simplest and leads to

$$F_{\alpha'\alpha}(\overline{\mathbf{K}},\mathbf{K}^*)=2(\tfrac{1}{3})^{3/2}(K_y^*)^3\left\{\exp(\sqrt{1/5}\overline{\mathbf{K}}\cdot\mathbf{K}^*)-\left[1+\frac{4}{\sqrt{45}}(\overline{\mathbf{K}}\cdot\mathbf{K}^*-\overline{K}_yK_y^*)\right]\exp(-\sqrt{1/45}\overline{\mathbf{K}}\cdot\mathbf{K}^*)\right\}\ . \tag{A5}$$

The key to the calculation of the overlap (A1) involves the expansion of $F_{\alpha'\alpha}(\overline{\mathbf{K}},\mathbf{K}^*)$ in terms of $\overline{\mathbf{K}}$ and $\mathbf{K}^*$-space polynomials. Substituting Eq. (A3) into (A2) and using SU(3) recoupling techniques

$$F_{\alpha'\alpha}(\bar{\mathbf{K}},\mathbf{K}^*)=\sum_{Q(\lambda_0\mu_0)\alpha_0}[P^{(Q-3,0)}(\bar{\mathbf{K}})\times P^{(0Q)}(\mathbf{K}^*)]^{(\lambda_0\mu_0)}_{\alpha_0}$$
$$\times\sum_{(\lambda\mu)}d(\lambda\mu)\left[\frac{d(\lambda_0\mu_0)}{d(10)d(40)d(Q0)}\right]^{1/2}\langle(\lambda_0\mu_0)\alpha_0,(01)\alpha'|(04)\alpha\rangle$$
$$\times U((0,Q-3)(\lambda\mu)(\mu_0\lambda_0)(40);(01)(Q0))\mathcal{O}^{Q(\lambda\mu)}\ , \tag{A6}$$

where $d(\lambda\mu)=(\lambda+1)(\mu+1)(\lambda+\mu+2)/2$ is the dimension of the SU(3) representation $(\lambda\mu)$, and the SU(3) Racah or U coefficients[10] are given in unitary form. Possible SU(3) labels in Eq. (A6) are $(Q-3,1)$ and $(Q-4,0)$ for $(\lambda\mu)$, and (03) and (14) for $(\lambda_0\mu_0)$. On the other hand, the expansion of $F_{\alpha'\alpha}(\bar{\mathbf{K}},\mathbf{K}^*)$, in the form (A5), is carried out in a Cartesian basis using the following formulas (see, e.g., Ref. 7),

$$(K_y^*)^3(\bar{\mathbf{K}}\cdot\mathbf{K}^*)^{Q-3}=-\left[\frac{Q!(Q-3)!d(Q0)}{d(30)}\right]^{1/2}[P^{(Q-3,0)}(\bar{\mathbf{K}})\times P^{(0Q)}(\mathbf{K}^*)]^{(03)}_{3(3/2)(3/2)}\ ,$$
$$\bar{K}_yK_y^*(\bar{\mathbf{K}}\cdot\mathbf{K}^*)^{Q-4}=-\left[\frac{Q!(Q-3)!d(Q-3,0)}{d(10)d(40)}\right]^{1/2}\sum_{(\lambda_0\mu_0)\alpha_0}[d(\lambda_0\mu_0)]^{1/2}\langle(\lambda_0\mu_0)\alpha_0,(01)\alpha'|(04)\alpha\rangle \tag{A7}$$
$$\times U((Q-3,0)(0,Q-4)(\lambda_0\mu_0)(04);(10)(0Q))$$
$$\times[P^{(Q-3,0)}(\bar{\mathbf{K}})\times P^{(0Q)}(\mathbf{K}^*)]^{(\lambda_0\mu_0)}_{\alpha_0}\ .$$

Combining Eqs. (A5)–(A7) leads to a linear equation with two unknowns $\mathcal{O}^{Q(Q-3,1)}$ and $\mathcal{O}^{Q(Q-4,0)}$. With explicit expressions for the U coefficients involved we get

$$\mathcal{O}^{Q(Q-4,0)}=\tfrac{2}{3}[\tfrac{1}{3}Q(Q+1)(Q+2)]^{1/2}[1-9(-\tfrac{1}{3})^{Q-3}](\tfrac{1}{5})^{(1/2)(Q-3)}\ ,$$
$$\mathcal{O}^{Q(Q-3,1)}=\tfrac{1}{3}[\tfrac{1}{3}(Q+1)(Q+2)(Q+3)]^{1/2}[1+(4Q-13)(-\tfrac{1}{3})^{Q-3}](\tfrac{1}{5})^{(1/2)(Q-3)}\ . \tag{A8}$$

[1] K. Ikeda *et al.*, Prog. Theor. Phys. Suppl. **68**, 1 (1980).
[2] H. Horiuchi, Prog. Theor. Phys. **51**, 745 (1974).
[3] Y. Suzuki, Prog. Theor. Phys. **55**, 1751 (1976); **56**, 111 (1976).
[4] S. Saito, Prog. Theor. Phys. **41**, 705 (1969).
[5] See, e.g., D. J. Rowe, Rep. Prog. Phys. **48**, 1419 (1985).
[6] K. T. Hecht, E. J. Reske, T. H. Seligman, and W. Zahn, Nucl. Phys. **A356**, 146 (1981).
[7] Y. Suzuki and K. T. Hecht, Nucl. Phys. **A455**, 315 (1986).
[8] Y. Suzuki, Nucl. Phys. **A470**, 119 (1987).
[9] Y. Suzuki, Nucl. Phys. **A448**, 395 (1986).
[10] J. P. Draayer and Y. Akiyama, J. Math. Phys. **14**, 1904 (1973); Y. Akiyama and J. P. Draayer, Comput. Phys. Commun. **5**, 405 (1973).
[11] A. Volkov, Nucl. Phys. **74**, 33 (1965).
[12] D. M. Brink and E. Boeker, Nucl. Phys. **A91**, 1 (1967).
[13] F. Ajzenberg-Selove, Nucl. Phys. **A460**, 1 (1986).
[14] M. G. Vassanji and D. J. Rowe, Phys. Lett. **125B**, 103 (1983).
[15] J. Broeckhove, Phys. Lett. **109B**, 5 (1982).
[16] K. T. Knöpfle, G. J. Wagner, H. Breuer, M. Rogge, and C. Mayer-Böricke, Phys. Rev. Lett. **35**, 779 (1975).
[17] M. N. Harakeh *et al.*, Nucl. Phys. **A265**, 189 (1976).
[18] K. T. Knöpfle *et al.*, Phys. Lett. **74B**, 191 (1978).
[19] A. Faessler, D. J. Millener, P. Paul, and D. Strottman, Nucl. Phys. **A330**, 333 (1979).
[20] S. S. Hanna *et al.*, Phys. Rev. Lett. **32**, 114 (1974).
[21] K. A. Snover, E. G. Adelberger, and D. R. Brown, Phys. Rev. Lett. **32**, 1061 (1974).
[22] A. Hotta, K. Itoh, and T. Saito, Phys. Rev. Lett. **33**, 790 (1974).
[23] F. Zwarts, A. G. Drentje, M. N. Harakeh, and A. van der Woude, Nucl. Phys. **A439**, 117 (1985).
[24] T. Hoshino and A. Arima, Phys. Rev. Lett. **37**, 266 (1976).
[25] S. Krewald, J. Birkholz, A. Faessler, and J. Speth, Phys. Rev. Lett. **33**, 1386 (1974).
[26] T. Ogawa, Y. Suzuki, and K. Ikeda, Prog. Theor. Phys. **57**, 1072 (1977).
[27] H. Kazama, K. Kato, and H. Tanaka, Prog. Theor. Phys. **75**, 571 (1986); **71**, 215 (1984).